

## Article

# Two Species of the Family Cyatholaimidae (Nematoda: Chromadorida) from Korea <sup>†</sup>

Hyeonggeun Kim <sup>1,2</sup>  and Raehyuk Jeong <sup>2,3,4,\*</sup> 

<sup>1</sup> Biodiversity Research Department, National Institute of Biological Resources, Incheon 22689, Republic of Korea; playing17@korea.kr

<sup>2</sup> Department of Environmental Science, Hanyang University, Seoul 04763, Republic of Korea

<sup>3</sup> Center for Creative Convergence Education, Hanyang University, Seoul 04763, Republic of Korea

<sup>4</sup> Research Institute of Natural Science, Hanyang University, Seoul 04763, Republic of Korea

\* Correspondence: rhjeong88@hanyang.ac.kr

<sup>†</sup> Zoobank: urn:lsid:zoobank.org:pub:8F0707D0-B7C1-4B32-8FC1-2C0BA3196259.

**Abstract:** During a survey of the Wando-gun rockpool area in Korea, two species belonging to the family Cyatholaimidae were discovered within a sponge, *Hymeniacidon sinapium*, and are hereby reported. Despite the monophyletic nature of the family Cyatholaimidae, it has been a topic of discussion among nematologists due to its lack of synapomorphic characteristics and overlapping generic diagnoses. Many genus-defining features consist of a combination of non-unique characters, which may not hold significant taxonomic importance. Consequently, most genera within the family are non-monophyletic according to phylogenetic findings. The absence of molecular data complicates the identification of taxonomically important characteristics that may have been previously overlooked. While the pore complex and the lateral pore-like structure have been suggested as potentially important traits, these insights are lacking in most recorded species, along with molecular data to confirm their significance in topology. Given the considerable amount of work required from the ground up, this study provides both morphological information (including taxonomic description, morphometric measurements, tabular key comparing key features to all valid congeners, illustration, and microscope photographs) and molecular data (partial sequences of three molecular regions, K2P distance comparison, and phylogenetic trees) for the two species discovered in Korea. The study also offers insights on potentially significant traits, such as the pore complex and other pore structures. The Korean specimen of *Acanthonchus* (*Seuratiella*) *tridentatus* resembles the original description regarding aspects such as the number and type of preloacal supplements, as well as the shape of the spicules and gubernaculum. However, variations are observed in the following characteristics: body ratio, nerve ring location, pharynx length, and the presence or absence of the ocelli. Our partial molecular sequences of the specimens also match identically with a single existing entry on NCBI identified as *A. (S.) tridentatus*. The new species, *Paracanthonchus spongius* sp. nov., is most similar to *P. kamui* in terms of the general shape of the body and gubernaculum but can be distinguished by differences in the number of preloacal supplements, amphid position, and gubernaculum ratio. The phylogenetic tree constructed based on the 28S rRNA region shows both species grouped within the monophyletic clade of Cyatholaimidae with high bootstrap support. However, achieving generic resolution of these species will require more molecular sequences of congeners to accumulate in the future.



**Citation:** Kim, H.; Jeong, R. Two Species of the Family Cyatholaimidae (Nematoda: Chromadorida) from Korea. *Diversity* **2023**, *15*, 1047. <https://doi.org/10.3390/d15101047>

Academic Editors: Michael Wink and Alexandra Teodósio

Received: 30 August 2023

Revised: 27 September 2023

Accepted: 27 September 2023

Published: 28 September 2023



**Copyright:** © 2023 by the authors. Licensee MDPI, Basel, Switzerland. This article is an open access article distributed under the terms and conditions of the Creative Commons Attribution (CC BY) license (<https://creativecommons.org/licenses/by/4.0/>).

**Keywords:** free-living marine nematode; meiofauna; Cyatholaimidae

## 1. Introduction

The nematode family Cyatholaimidae Filipjev, 1918, is a diverse group of free-living marine nematodes that inhabit various habitats, including subtidal and intertidal zones, as well as the deep sea [1]. This relatively large family, which comprises 27 genera and

258 species [2], has posed challenges for species identification due to its large roster of species and lack of distinct morphological synapomorphies for species characterization [3]. Recently, there have been numerous discoveries and molecular phylogenetic analyses involving this family [1–3], yielding new insights that suggest the potential significance of the pore complex in species identification [3,4]. These findings further indicate the necessity to redefine cyatholaimid subfamilies [2,3]. Since the recent discovery of *Paracanthonchus yeongjongensis* by Kim, Lee & Jeong, 2023 from Yeongjongdo Island, Incheon, Korea, two additional species of Cyatholaimidae have been found in an intertidal rockpool at Sinji-Do, Wando-gun in Korea. Both species were retrieved from a sponge known as *Hymeniacidon sinapium*, which is widespread along the entire coast of Korea. This orange-colored sponge is typically found attached to rocks in an intertidal zone. Upon close inspection, it is evident that the sponge serves as a habitat not only for nematodes but also for various macro and meiofaunal organisms (e.g., Isopoda and Polychaeta). To date, approximately 80 species of free-living marine nematodes have been reported in Korea, all of which have been found either in intertidal zones or on macroalgae. While free-living marine nematodes have been discovered within sponges [5–7], this is the first record for it to be discovered within *H. sinapium*.

The genus *Acanthonchus* Cobb, 1920 was initially established with the type species *A. viviparus*, and its two subgenera were erected in 1955 by Wieser, when he noticed the close resemblance between the genera *Acanthonchus* and *Seuratiella*, the latter of which was originally established by Ditlevsen 1921 with the type species *Seuratiella gracilis*. Wieser (1955) distinguished the two subgenera by the absence and presence of equal-sized teeth (*Acanthonchus* and *Seuratiella*, respectively) but was doubtful in doing so, noting that the character differences are very subtle and that the two subgenera may eventually be considered synonymous in the future [8]. Currently, there are ten recognized species of *Acanthonchus* worldwide, and the validity of the two subgenera is maintained primarily by convention. The most recent addition to the genus, *Acanthonchus singaporensis*, is not assigned to a subgenus [9]. Whether this omission was intentional on the part of the authors remains uncertain, but the ambiguity and potential synonymy of the two subgenera require investigation and resolution in the future. Among the 27 genera within the family Cyatholaimidae, *Acanthonchus* is the only genus with a subgenus, and it can be discerned by the anterior-most supplement (much larger comparatively, almost double in size). The genus can be characterized by the following features: (1) cuticle with lateral differentiation either absent or present in larger and more widely spaced dots, (2) tubular pre-cloacal supplements, and (3) gubernaculum paired, usually dilated and dentated distally [1].

The genus *Paracanthonchus* was first established by Micoletzky in 1924, with type species *Paracanthonchus caecus*. This large genus comprises many cosmopolitan species and currently has 60 valid species recorded worldwide [2]. The combination of morphological keys that defines this genus overlaps with the diagnostic keys of other species belonging to the family Cyatholaimidae, making species identification of this specific family a challenging task [1,2]. Until recent efforts by Miljutina & Miljutin, 2015 and Kim, Lee & Jeong, 2023 to update the genus [2,10], discrepancies existed even in defining the total number of reported species [11–13]. *Paracanthonchus* has been noted as being one of the most problematic genera within the family Cyatholaimidae, which requires updating both morphologically and molecularly [1–3]. Currently lacking proper synapomorphic characters, *Paracanthonchus* serves almost as a ‘sanctuary’ encompassing all non-specific cyatholaimids. With most species of the genus being described prior to the millennium, most species lack molecular data to test their non-monophyletic nature. As molecular data for these species gradually accumulate, it is expected that a significant number of species will be either synonymized or reclassified into new or existing genera.

Despite being such a diverse and widely distributed family, only four cyatholaimids (*Marylynnia denticulata*, *P. yeongjongensis*, *Paracanthonchus macrodon*, and *Paracanthonchus kamui*) have been reported in Korea. *Marylynnia* was found in sublittoral mud, *P. yeongjongensis* in intertidal mud, and the remaining two *Paracanthonchus* were collected from

macroalgae. In this study, we report two cyatholamids (*Paracanthonchus spongius* sp. nov. and *Acanthonchus* (*Seuratiella*) *tridentatus*) collected from intertidal sponges in Korea. We are providing both morphological information (including an updated diagnosis, species description, line drawing, morphometrics table, tabular key, and remarks) and molecular data (partial sequences of three marker regions: mtCOI, 18S, and 28S rRNA) for these two species. Additionally, our morphological analysis includes insights into potentially important characters, such as pore complex and lateral pore-like structures [1,3,4], which require further investigation to understand their true taxonomic significance in cyatholaimids.

## 2. Materials and Methods

### 2.1. Morphological Analysis

Free-living marine nematodes were collected by rinsing sponges (*Hymeniacidon sinapium*) found in rock pools at Sinji-Do, Wando-gun, Korea on 11 April 2023 (Figure 1). The collected substrates, which included meiofauna and macrofauna, were fixed with two different fixatives: 90% ethanol for molecular analysis (to prevent morphological changes), and 5% formol solution for morphological analysis. Samples were brought back to the laboratory to be observed, and were stored in a refrigerator or freezer, depending on the type of fixative used.

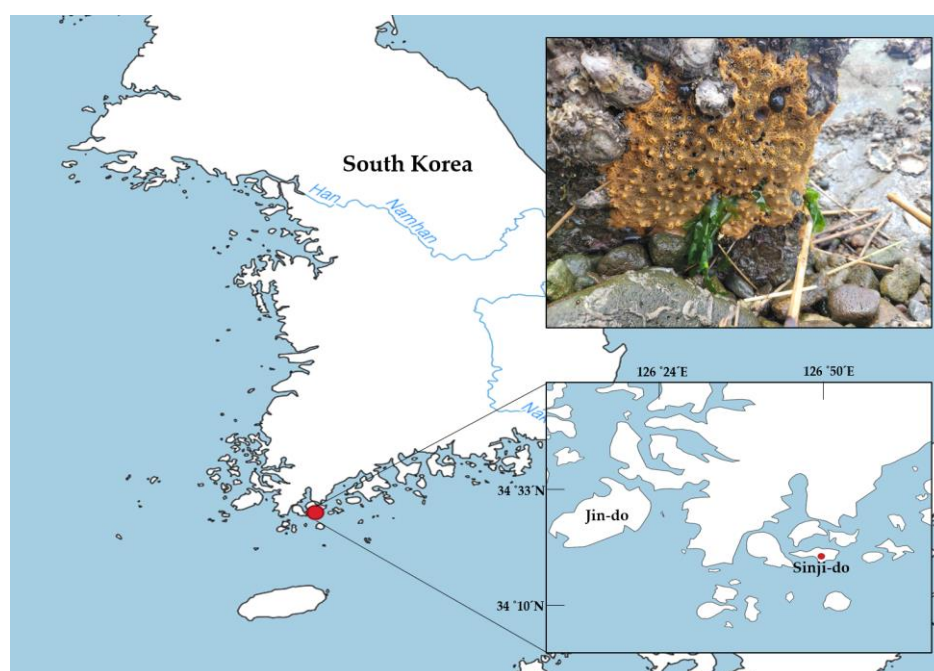


**Figure 1.** Sample locality of *Acanthonchus* (*Seuratiella*) *tridentatus* and *Paracanthonchus spongius* sp. nov. and photograph of the sponge it was retrieved from, *Hymeniacidon sinapium*.

Nematode specimens of interest were sorted to a single-welled Petri dish under a dissecting microscope (Olympus SZX-10, Tokyo, Japan). Nematodes were transferred to a well containing a solution of 10% glycerol and distilled water, to be dehydrated for 1 to 2 days, after which they were mounted with microscopic glass beads on anhydrous glycerin using the standard wax-ring method [14]. Following slide preparation, each specimen was observed under 100× objective lens with immersion oil using an optical microscope (Nikon Eclipse 80i, Tokyo, Japan) with Nomarski Differential Interference Contrast (DIC) illumination for species identification. Line drawings were prepared digitally with an iPad (Apple, Cupertino, CA, USA) and Adobe Illustrator (Adobe, San Jose, CA, USA). All measurements were made with Fiji software [15]. The classification of nematodes is based on Hodda (2022) [16], and species identification guided by pictorial keys provided by Platt and Warwick (1988) [17].

## 2.2. gDNA Extraction and Amplification

To begin DNA extraction, specimens were handpicked from samples fixed with 90% ethanol, and transferred to a pool of distilled water to be washed of excess ethanol. For extraction of genomic DNA, DNAeasy Blood & Tissue Kit (Qiagen, Hilden, Germany) was used following manufacturer's instructions. DNA concentration was measured using NanoDrop 2000 (ThermoScientific, Wilmington, NC, USA), to which concentrations ranged from 2.5 to 4.5 ng/ $\mu$ L. For DNA amplification, AccuPower<sup>®</sup> PCR Master Mix (Bioneer, Daejeon, Korea) was used, with 20  $\mu$ L of total reaction volume as suggested by the manufacturer: components of total reaction are as follows: 10  $\mu$ L premix, 1  $\mu$ L for each primer (0.33–0.62  $\mu$ M in concentration, depending on the primer), 6  $\mu$ L DNA template, and 2  $\mu$ L ultra-pure water. The MtCOI gene was amplified using JB3 (5'-TTTTTGGGCATCCTGAGGTTTAT-3') and JB5 (5'-AGCACCTAAACTTAAAACATAATGAAAATG-3') primers. The amplification protocol involved an initial denaturation at 94 °C for 5 min, followed by 5 cycles of denaturation at 94 °C for 30 s, annealing at 54 °C for 30 s, and extension at 72 °C for 30 s. This was followed by 35 cycles of denaturation at 94 °C for 30 s, annealing at 50 °C for 30 s, and extension at 72 °C for 30 s, concluding with a final extension step at 72 °C for 10 min [18]. For the partial 18S rRNA gene amplification, 18F-CL-F (5'-TCAAAGATTAAGCCATGCAT-3') and 530R (5'-GCGGCTGCTGGCACCACACTT-3') primers were used. The amplification process involved an initial denaturation at 95 °C for 3 min, followed by 36 cycles of denaturation at 95 °C for 30 s, annealing at 50 °C for 45 s, and extension at 72 °C for 3 min, with a final extension step at 72 °C for 7 min [19,20]. For the amplification of the D2-D3 region, D2A (5'-ACAAGTACCGTGAGGGAAAGTTG-3') and D3B (5'-TCGGAAGGAACCAGCTACTA-3') primers were used. The amplification protocol started with an initial denaturation at 95 °C for 5 min, followed by 37 cycles of denaturation at 95 °C for 30 s, annealing at 56 °C for 1 min, and extension at 72 °C for 1 min 30 s. The process concluded with a final extension step at 72 °C for 5 min [21]. PCR products were visually checked using 1% agarose gel electrophoresis to confirm amplification success. PCR products were subject to purification and sequencing at Bioneer (Korea). All newly acquired sequences from this research have been submitted to GenBank (Table 1).

**Table 1.** GenBank accession numbers of sequences obtained in this study. (“–” indicates unsuccessful amplification).

Specimen	Species Name	Voucher Number	GenBank Accession Number		
			mtCOI	18S	D2-D3
			JB3	18S-CL-F	D2A
			/JB5	/530R	/D3B
			(~390 bp)	(~500 bp)	(~730 bp)
1	<i>Acanthonchus (Seuratiella) tridentatus</i>	A3	OR606577	–	–
2	<i>Acanthonchus (Seuratiella) tridentatus</i>	A4	OR606578	–	–
3	<i>Acanthonchus (Seuratiella) tridentatus</i>	B2	OR606579	OR606555	OR606562
4	<i>Acanthonchus (Seuratiella) tridentatus</i>	C4	OR606580	–	OR606563
5	<i>Acanthonchus (Seuratiella) tridentatus</i>	D1	OR606581	OR606556	–
6	<i>Acanthonchus (Seuratiella) tridentatus</i>	D2	OR606582	OR606557	–
7	<i>Acanthonchus (Seuratiella) tridentatus</i>	D3	–	–	OR606564
8	<i>Acanthonchus (Seuratiella) tridentatus</i>	D4	OR606583	OR606558	–
9	<i>Acanthonchus (Seuratiella) tridentatus</i>	D5	OR606584	OR606559	–
10	<i>Acanthonchus (Seuratiella) tridentatus</i>	D6	OR606585	OR606560	OR606565
11	<i>Paracanthonchus spongius</i> sp. nov.	A8	OR606586	–	–
12	<i>Paracanthonchus spongius</i> sp. nov.	E1	OR606587	–	OR606566
13	<i>Paracanthonchus spongius</i> sp. nov.	E2	OR606588	OR606561	OR606567
14	<i>Paracanthonchus spongius</i> sp. nov.	E4	–	–	OR606568

### 2.3. Phylogenetic Analysis

Molecular sequences were visualized utilizing FinchTV (v. 1.4.0, Geospiza, Inc.; Seattle, WA, USA; <http://www.geospiza.com>; accessed on 1 April 2023), and any low-quality peaks were eliminated through a comparison of both complementary strands. The forward and reverse strands were aligned using ClustalW [22], a tool embedded in MEGA (v. 11.0.13) [23,24]. These aligned sequences were then subjected to comparison with the NCBI GenBank database using the BLAST algorithm [25]. Pairwise distances between interspecies, and closely related species were calculated for mtCOI, 18S, and 28S rRNA sequences using the K2P model in MEGA 11 [26]. Phylogenetic trees were constructed based on 28S rRNA sequences.

Maximum likelihood (ML) and Bayesian inference (BI) approaches were used to build phylogenetic tree using the 28S rRNA sequences. For the ML analysis, IQ-Tree (multicore v.2.0.3) [27] in combination with the ModelFinder tool [28] was used to determine the best-fit model using Akaike information criterion (AIC). GTR + F + G4 model was determined to be the best-fitting model for 28S dataset and subsequently chosen to construct the ML trees using the IQ-Tree web servers, using the ultrafast settings with 1000 bootstrap replicates [27]. For the BI analysis, the best-fit model was determined using jModelTest software (v. 2.1.7) [29], and the tree was generated using the MrBayes software (v. 3.2.6) [30]. The model parameters for the 28S rRNA dataset were set as follows: Lset base = (0.2310, 0.2349, 0.3051, 0.2290) nst = 6 rmat = (0.6209, 1.6180, 1.0000, 0.6209, 4.1959, 1.0000) gamma shape = 0.4690 ncat = 4 pinvar = 0 with *Enoploides* sp. set as outgroup. Markov Chain Monte Carlo (MCMC) was run with ngen = 1,000,000, nchains = 4, samplefreq = 100, savebrlens = yes, printfreq = 1000, sump burnin = 250, and sumt burnin = 250. All trees were exported to FigTree (v. 1.4.4) [31] where visualizations and modifications were made.

## 3. Results

### 3.1. Morphological Analysis

#### Systematics

Class Chromadorea Inglis, 1983

Order Chromadorida Chitwood, 1933

Family Cyatholaimidae Filipjev, 1918 (De-Coninck & Schuurmans-Stekhoven, 1933)

Subfamily Paracanthonchiinae De-Coninck, 1965

Genus *Acanthonchus* Cobb, 1920

Subgenus *Acanthonchus* (*Seuratiella*) (Ditlevsen, 1921) Wieser, 1955

**Diagnosis** (Followed Tchesunov 2014 and Cunha et al., 2022)

Cyatholaimidae. Paracanthonchiinae. Body cuticle composed of transverse rows of tiny fine dots, which may be laterally larger or absent. Six outer labial and four cephalic setae jointed in a one circle. Amphideal fovea multi-spiral. Buccal cavity with dorsal distinct tooth or absent (weakly development). Gubernaculum proximally paired, distally dentate. Tubular precloacal supplements, which anterior-most much larger than the other.

Type species: *Acanthonchus* (*Acanthonchus*) *viviparus* Cobb, 1920

#### List of valid species

1. *Acanthonchus* (*Acanthonchus*) *arcuatus* (Kreis, 1928) Wieser, 1955 (Kreis, 1928: 18–20, Taf. IV, Figure 9a–f; Italy, Tarmina, intertidal, algae) [32].
2. *Acanthonchus* (*Acanthonchus*) *cobbi* Chitwood, 1951 (Chitwood, 1951: 639, Figure 7D,E; USA, Texas, Rockport Harbor, Piling, 1 m depth) [33].
3. *Acanthonchus* (*Acanthonchus*) *duplicatus* Wieser, 1959 (Wieser 1959: 42–43, Figure 42a,b; USA, Seattle, Vashon Island, fine to medium fine sand) [34].
4. *Acanthonchus* (*Acanthonchus*) *setoi* Wieser, 1955 (Wieser 1955: 8–9, Figure 3a,b; Japan, Shirahama, from Sargassum on the rocks below water mark) [8].
5. *Acanthonchus* (*Acanthonchus*) *viviparus* Cobb, 1920 (Cobb 1920: 321–323, fig 101; California, San Pedro, mud. Allgén 1947: 142, Figure 45; California, San Pedro, harbor) [35].

6. *Acanthonchus (Seuratiella) gracilis* (Ditlevsen, 1918) Wieser, 1955 (Ditlevsen 1918: 197–198, Pl. V, Figures 1 and 9; Pl. VII, Figure 7; Denmark, among algae and hydrozoa on stones) [36].
7. *Acanthonchus (Seuratiella) pugionatus* Vitiello, 1970 (Vitiello 1970: 474–475, Pl. VIII, Figure 17a–d; France, gulf of Marseille, 320 m depth, mud) [37].
8. *Acanthonchus (Seuratiella) rostratus* Wieser, 1959 (Wieser 1959: 41–42, Figure 41a,b; USA, Seattle, Golden Gardens, medium fine to coarse sand, 0.5 m–1.5 m depth) [34].
9. *Acanthonchus (Seuratiella) singaporensis* Chen Cheng-Ann, Nguyen Dinh Tu & Smol, 2015 (Chen et al., 2015: 71–73, Figures 3 and 4; Singapore, Paulo Ubin, Tanjung Tajam rocky area) [9].
10. *Acanthonchus (Seuratiella) tridentatus* Kito, 1976 (Kito 1976: 570–573, Figure 2; Japan, Oshoro, on Sargassum in the subtidal zone. This study:) [38].

#### Tabular key to valid species (Table 2)

The tabular key consists of all ten valid species included within the genus, and all measurements were corrected (if erroneous) by reviewing original and related papers.

#### Description

*Acanthonchus (Seuratiella) tridentatus* Kito, 1976. (Figures 2 and 3, Table 3)

**Locality:** collected from *Hymeniacidon sinapium*, on subtidal rocky zone (34°19'28" N, 126°49'50" E), Sinji-Do, Wando-Gun, Korea

**Materials examined:** 3♂♂ (NIBRIV0000909790, NIBRIV0000909791, NIBRIV0000909792), 2♀♀ (NIBRIV0000909793, NIBRIV0000909794), each specimen on each slide from rocky zone (34°19'28" N, 126°49'50" E) on 11 April 2023

#### Description:

**Male:** Body generally cylindrical, gradually widening from the anterior end of head to the ocelli and then tapering from the anus to the tail (Figure 2A,B). Cuticle clearly ornamented with transverse rows of punctations spanning the entire body. Punctations evenly distributed, with slightly lateral differentiation at the head and the tail region with regularly slightly larger-sized punctation (Figure 2C,F). Four longitudinal rows of hypodermal pores, referred to as the pore complex (PC), vertically present from under the amphid to the tail end (Figure 2C–F). Six outer labial setae and four cephalic setae arranged in one circle on the head, all similar in length, about 4.5 µm long (Figure 2C). Several somatic setae are present all over the body. Amphids positioned in the middle from the tip of the head to the ocelli, multispiral with 2.5–3 turns and a width of 7.5 µm (Figure 2C,D). Two somatic setae located below the amphid, and, just below that, two ocelli are present, which appear to overlap. Buccal cavity shallow (showing only a single row connected to the esophagus). Dorsal tooth underdeveloped (sublateral teeth not observed). The nerve ring situated slightly below the midpoint of the pharynx, and 113 µm from the anterior edge (Figure 2C,D). Pharynx cylindrical, and the bulb not well-developed. Cardia not readily observed. The reproduction system clearly diorchic, opposed, and outstretched, the anterior part about 1.5 times longer than the posterior part (Figure 2A). The spicule curved and paired, 43 µm long, initially appearing slightly bent and tapering to a pointed end. The gubernaculum paired, 35 µm long, spear-like shape in the anteriorly and expanding towards the distal part. At the distal end of gubernaculum, numerous rows of denticle appearing as two lines of a circle, with larger denticles at the lower part (Figure 2E). Three pre-anal setae arranged in two rows below the anus. Six pre-anal supplements present. The size of the first supplement 32.5 µm long, and the second 20 µm long. Distance between each supplement gradually increases toward the anterior part. The most anterior and posterior supplements located at distances of 8.5 µm and 115 µm from the anus, respectively. The fifth and sixth supplements very small and vaguely observed (especially the sixth). All supplements, except the last two, heavily cuticularized. Cell bodies of three caudal glands are present. Tail conical and short, 130 µm long (Figure 2E).

**Female:** Similar to males in basic features, such as the cuticle patterns, the shape of buccal cavity, and the body shape; however, the body length is generally longer than males.

The body length is 1991  $\mu\text{m}$ . The ovaries are didelphic, two opposed, and outstretched. The vulva is located at 47% of the body length, 944  $\mu\text{m}$  from the anterior end (Figure 2G).

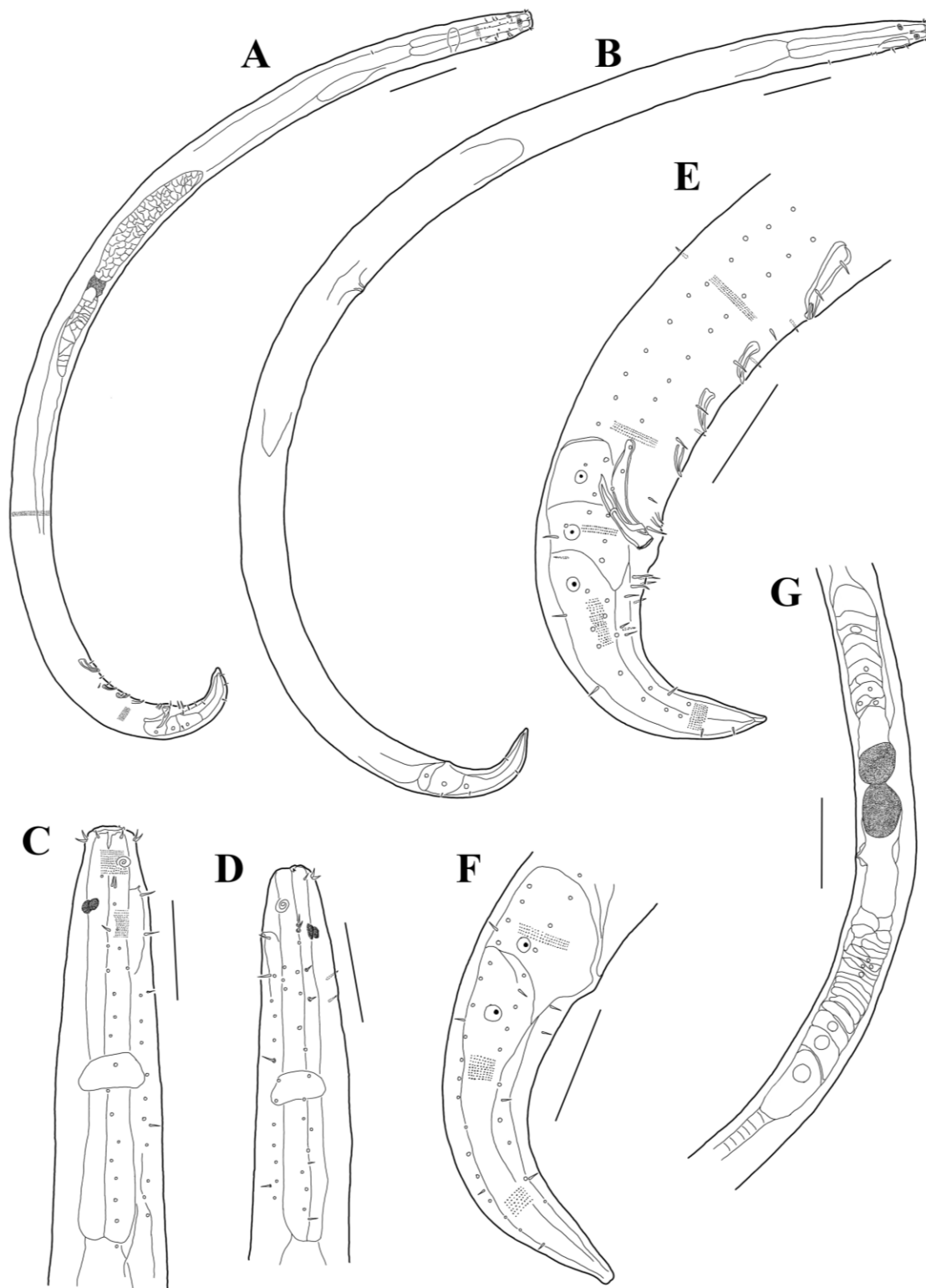


**Figure 2.** *Acanthonchus (Seuratiella) tridentatus*—**A**, male habitus; **B**, female habitus; **C**, female anterior region; **D**, male anterior region; **E**, male cloacal region; **F**, female cloacal region; **G**, female reproductive system. Scale bars: **A,B,G** = 100  $\mu\text{m}$ ; **C-F** = 50  $\mu\text{m}$ .

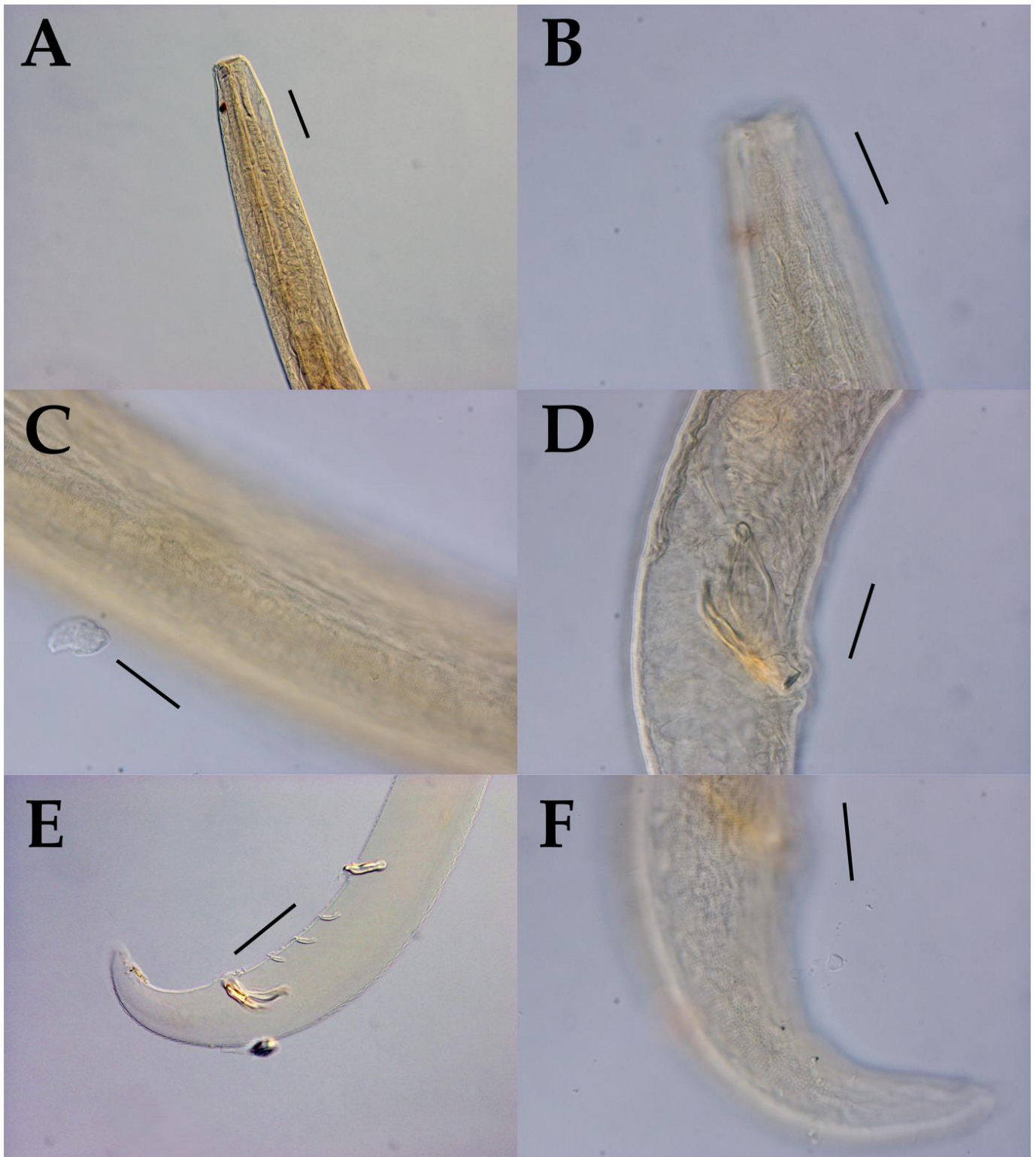


**Figure 3.** *Acanthonchus (Seuratiella) tridentatus*—(A) anterior part with pharynx and ocelli, male; (B) cuticle ornamentation at the head with amphid, male; (C) cuticle ornamentation at the mid-body, male; (D) spicule and gubernaculum, male; (E) tail region with cloacal supplements, male; (F) tail region with lateral differentiation, male. Scale bars: (A,E) = 30  $\mu\text{m}$ ; (B–D,F) = 20  $\mu\text{m}$ .

**Table 2.** Tabular key of valid *Acanthonchus* species with morphological characters (all measurements in  $\mu\text{m}$ ; “\*” indicates Korean specimens; “–” indicates unavailable information; “n/a” indicates not applicable).

Species	Body Length (Male)	Body Length (Female)	Lateral Differentiation of Cuticle	Development of Dorsal Tooth	Amphid Width	Turn Number of Amphid	Spicule Length as Arc	Gubernaculum Length	Number of Cusps on Distal End of Gubernaculum	Extension at the Distal End of Gubernaculum	Ocelli	Anterior Preanal Supplement Size	Difference in Size between First and Second Supplement	Number of Supplements	Tail Shape
<i>A. (A.) arcuatus</i>	1184	none	none	present	n/a	1.5	31	29	none	extended	none	14	less than 2×	5	conical-cylindrical or conical
<i>A. (A.) cobbi</i>	1300	1500	none	present	n/a	3.5	34	32	trifid claw with numerous denticles	extended	none	24	less than 2×	5	conical
<i>A. (A.) duplicatus</i>	1940	–	none	present	15	4	48	48	2 denticles	extended	none	54	over 2×	6	conical
<i>A. (A.) setoi</i>	1220	–	only posterior	present	12.2	4	26	27	numerous denticles	extended	none	30	over 2×	5	conical
<i>A. (A.) viviparus</i>	1300	1600	anterior/posterior	present	8	3.5	n/a	n/a	none	extended	none	n/a	over 2×	4	n/a
<i>A. (S.) gracilis</i>	1300	–	none	none	6	n/a	39	36	none	none	present	27	over 2×	4	conical
<i>A. (S.) pugionatus</i>	977	–	none	present	8.5	3.7–4.3	32	27	numerous denticles	extended	present	34	over 2×	6	conical
<i>A. (S.) rostratus</i>	1270–1540	1820	anterior/posterior	weakly present	9.5	2.75–3	46	42	none	extended	present	34	over 2×	6	conical
<i>A. (S.) singaporensis</i>	1209–1255	–	only posterior	weakly present	8.7–9.2	5.5	37	36–37	none	extended	none	36	over the 2×	6	conical
<i>A. (S.) tridentatus</i>	833–1350	810–1358	anterior/posterior	weakly present	5–8	3–3.3	34–40	26–37	two rows small point and three large	extended	none	26–31	2×	6	conical
<i>A. (S.) tridentatus</i> *	1662	1991	anterior/posterior	weakly present	6.8–7.5	2.5–3	43–46	35–36.5	numerous denticles	extended	present	32.5–35	less than 2×	6	conical

**Table 3.** Measurements of the Korean *Acanthonchus (Seuratiella) tridentatus* (all measurements in  $\mu\text{m}$ ; “–” indicates unavailable information; “n/a” indicates not applicable).

<i>Acanthonchus (Seuratiella) tridentatus</i> Kito, 1976					
Characters	Male 1	Male 2	Male 3	Female 1	Female 2
L	1622	1590	1597	1991	1750
hd	25	21	24	25	24
LSL	4.5	4.5	4.5	5	5
CSL	4.5	4.5	4.5	5	5
bcl	–	–	–	10	–
anterior to amp	17	16	n/a	15.5	n/a
amp	7.5	6.8	n/a	7	n/a
na	2.5	2.5	n/a	2.5	n/a
amp cbd	30	28	n/a	29	n/a
NL	113	108	104	123	101
ncbd	45	45.5	41.5	52.5	43.5
PL	177	185	177.5	206.5	190
pcbd	48.5	49	46.5	57.5	49
ep	32	32	n/a	31	n/a
Ocelli	present	present	present	present	present
mbd	57	57	57	67.5	66
VL	–	–	–	944	843
ov	–	–	–	617	621
abd	51.5	52	53	53	50
spia	43	46	46	–	–
gub	35	38	36.5	–	–
ns	6	6	6	–	–
dps	8.5	9.5	10	–	–
das	115	120	120.5	–	–
first supplement size	32.5	35.5	35	–	–
second supplement size	20	23.5	19	–	–
TL	130	132	130	160	151
a	28.5	27.9	28.0	29.5	26.5
b	9.2	8.6	9.0	9.6	9.2
c	12.5	12.0	12.3	12.4	11.6
c'	2.5	2.5	2.5	3.0	3.0
V	–	–	–	0.5	0.5
amp'	0.3	0.2	n/a	0.2	n/a
s'	0.8	0.9	0.9	–	–

**Systematics**Genus *Paracanthonchus* Micoletzky, 1923**Diagnosis** (Followed Tchesunov 2014)

Cyatholaimidae. Paracanthonchinae. Body cuticle composed of transverse rows of tiny fine dots, which laterally may be larger or irregularly arranged. Six outer labial and four cephalic setae jointed in one circle. Amphideal fovea multi-spiral. Cheilostom with twelve rugae. Buccal cavity with larger dorsal tooth and one or two pairs smaller subventral teeth. Gubernaculum proximally paired, distally expanded, and dentate. Tubular preloacal supplementary organs.

Type species: *Paracanthonchus caecus* (Bastian, 1865)**List of valid species**

Refer to Table S1 (an updated table from Kim, Lee &amp; Jeong, 2023 [2])

**Tabular key to valid species**

Refer to Table S1 (an updated table from Kim, Lee &amp; Jeong, 2023 [2])

**Description***Paracanthonchus spongius* sp. nov. (Figures 4 and 5, Table 4)

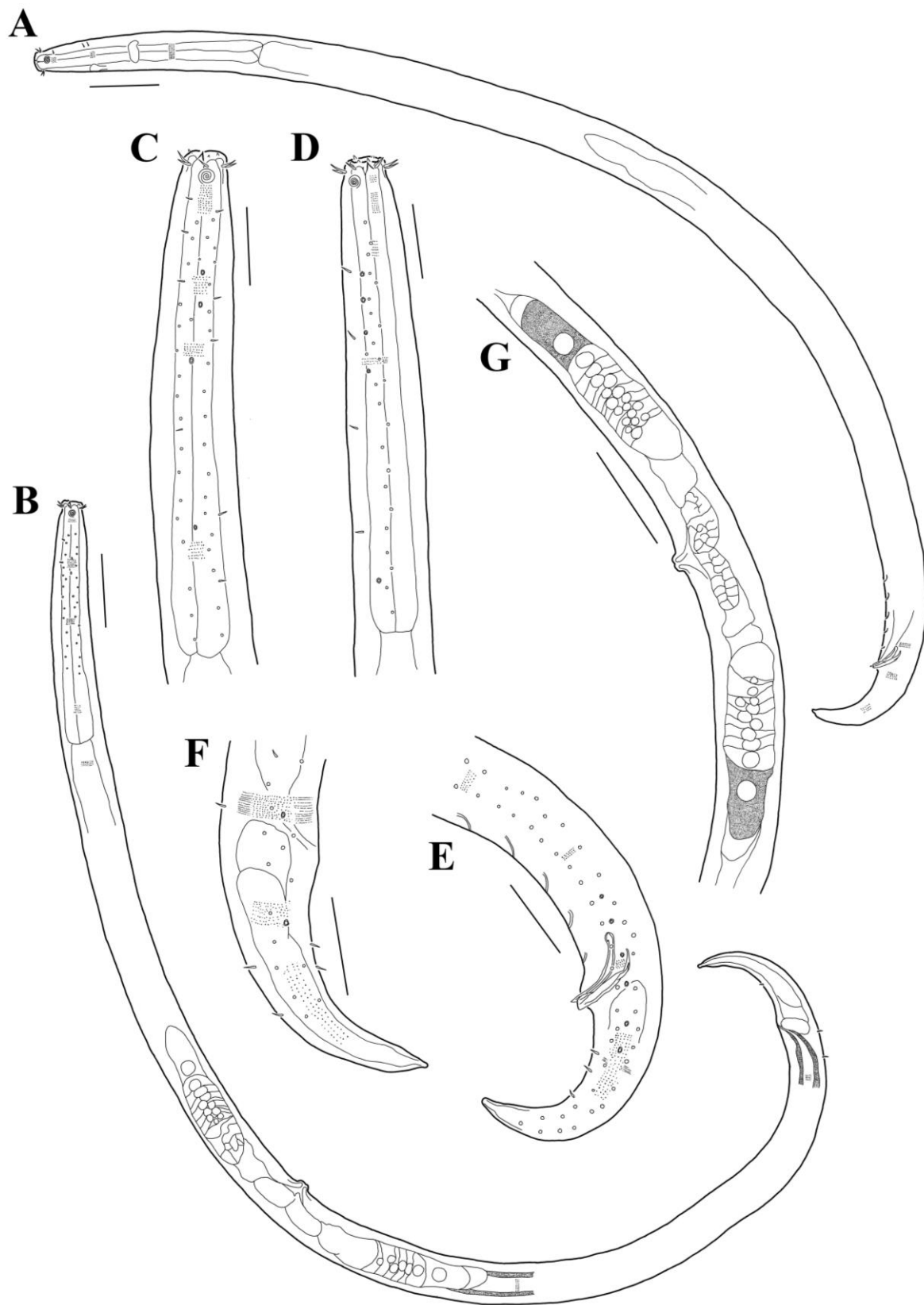


**Figure 4.** *Paracanthonchus spongius* sp. nov. —**A**, male habitus (holotype); **B**, female habitus (paratype); **C**, female anterior region (paratype); **D**, male anterior region (holotype); **E**, male cloacal region (holotype); **F**, female cloacal region (paratype); **G**, female reproductive system (paratype). Scale bars: (A,B,G) = 100  $\mu$ m; (C–F) = 50  $\mu$ m.

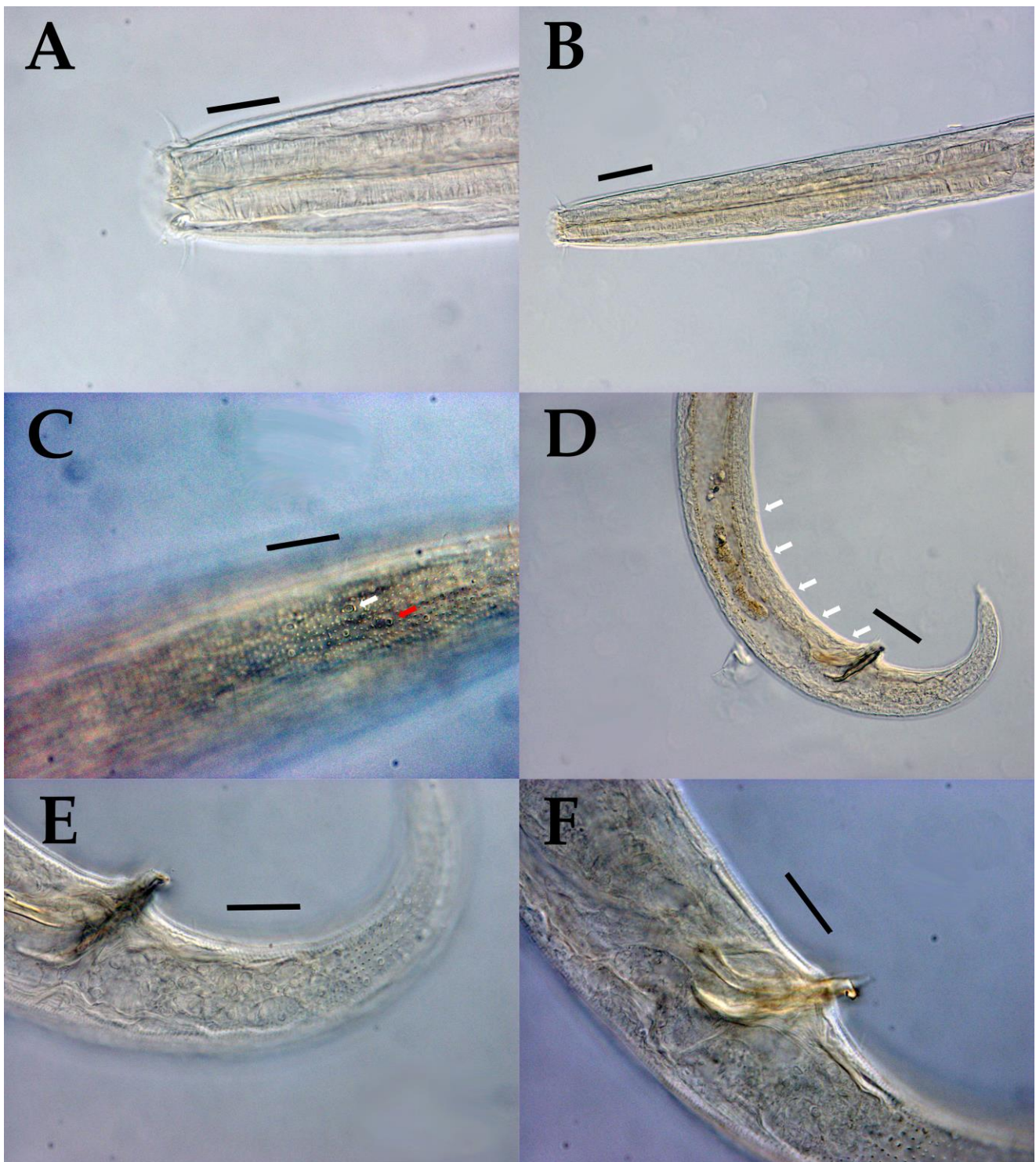


**Figure 5.** *Paracanthonchus spongicus* sp. nov.—(A) male, head with dorsal tooth and inner, outer labial setae (holotype); (B) male, pharynx region (holotype); (C) male, lateral differentiation at pharynx region (white arrow, LP; red arrow, PC) (paratype); (D) male, cloacal region (arrow, located at cloacal supplements) (holotype); (E) tail region with lateral differentiation (holotype); (F) male spicule and gubernaculum. Scale bars: (A,C,E,F) = 20  $\mu$ m; (B,D) = 30  $\mu$ m.

**Zoobank registration:**

urn:lsid:zoobank.org:act:E50FB4CD-12B6-4A47-851F-1E88F3170E92

**Locality:** collected from *Hymeniacidon sinapium*, on subtidal rocky zone (34°19'28" N, 126°49'50" E), Sinji-Do, Wando-Gun, Korea.

**Materials examined:** Holotype 1♂(NIBRIV0000909795) on one slide. Paratype 2♂♂ and 1♀(NIBRIV0000909796, NIBRIV0000909797, NIBRIV0000909798) on each slide all from subtidal rocky zone (34°19'28" N, 126°49'50" E) on 11 April 2023. Paratype 1♂ and 1♀(NIBRIV0000909799, NIBRIV0000909800) on each slide all from subtidal rocky zone (34°43'59" N, 127°44'57" E) on 20 October 2022.

**Etymology:** The species name *spongius* is given as the species was discovered off a sponge species, *Hymeniacidon sinapium*.

**Table 4.** Morphometric measurement of *Paracanthonchus spongius* sp. nov. (all measurements in µm; “–” indicates unavailable information; “n/a” indicates not applicable).

<i>Paracanthonchus spongius</i> sp. nov.			
Characters	Holotype	Paratype (m)	Paratype (f)
L	1793	1911	2145
hd	27.5	27	22.5
LSL	11.5	8.5	9
CSL	11.5	8.5	9
bcl	8	6	6
anterior to amp	9.3	12	8.7
amp	7.5	10	8
na	3.5	3.5	3.5
amp cbd	30	30	24.5
NL	150	144	n/a
ncbd	48	52	n/a
PL	315	325	255.5
pcbd	52	57	46
mbd	60	67	68
VL	–	–	1021
ov	–	–	570
abd	49.5	51.5	50
spia	51.5	49	–
gub	48.5	47	–
ns	5	5	–
dps	23	24.5	–
das	130	122	–
TL	136	153	157
a	29.9	28.5	31.5
b	5.7	5.9	8.4
c	13.2	12.5	13.7
c'	2.7	3.0	3.1
V	–	–	0.5
amp'	0.3	0.3	0.3
s'	1.0	1.0	–

#### Description:

**Male:** Body generally cylindrical, gradually increasing in size from the anterior end of the head to the nerve ring, and then tapering from the anus to the tail (Figure 4A,B). Cuticle clearly ornamented with transverse rows of punctations across the entire body. Punctuation generally distributed throughout the body, showing slight lateral differentiation. Particularly in the tail region, large-sized punctations irregularly arranged (Figure 4E,F). A vertical arrangement of hypodermal pores referred to as pore complex (PC) extends from just 40 µm below the anterior end of the head to the tail end. Additionally, lateral pore-like structure (LP) present from the head to the end of esophageal region, and in the tail region, both on the lateral side (Figure 4C–F), occurring sporadically in any other region. Six outer labial setae and four cephalic setae arranged in a single circle on the head, all similar in length, about 11.5 µm long (Figure 4C,D). Somatic setae ornament the body. Amphids positioned just below the labial setae region, multispiral with 3.5–4 turns, 7.5 µm in width, 30% of the amphid corresponding body diameter. Buccal cavity flattened and conical with

one dorsal tooth and a pair of sublateral teeth (whether in one or two pairs cannot be determined through observation). Ocelli absent. Nerve ring situated slightly above the midpoint of the esophagus, at 150  $\mu\text{m}$  from the anterior end. Pharynx cylindrical with a slightly developed bulb at the proximal part. Cardia not well observed. Reproduction system clearly diorchic, opposed, and outstretched, but observed with difficulty. Spicule curved and paired, 51.5  $\mu\text{m}$  long, tapering to a pointed end. Gubernaculum paired, 48.5  $\mu\text{m}$  long, with the proximal part a little curved in an L-shape and a pointed tip. The distal end not greatly expanded and bears numerous denticles. Five thin tubular pre-anal supplements present (Figure 4E). The distance between each supplement comparable, with only the size of fifth being smaller than the others. The most anterior and the posterior supplement 23  $\mu\text{m}$  and 130  $\mu\text{m}$  from the anus. Three caudal glands present.

Female: Similar to males in basic features, such as the cuticle patterns, the buccal cavity, and the body shape; however, the body length is longer in males. The body length is 2145  $\mu\text{m}$ . The ovaries are didelphic, two opposed, and reflexed (Figure 4G). The vulva is located 47% of the body length, 1021  $\mu\text{m}$  from the anterior end.

### 3.2. Molecular Analysis

A total of fourteen specimens were partially sequenced, including ten specimens of *A. (S.) tridentatus* and four specimens of *P. spongius* sp. nov. Despite targeting multiple regions (such as mtCOI, 18S, and 28S rRNA), the success of sequencing varied among these regions, and the amplification success seemed random among the specimens (sequencing success and the respective NCBI accession number are available in Table 1). In the compilation of our results, we successfully obtained sequences for all three regions of the two species under investigation. However, it is worth noting that the 18S rRNA sequence of *P. spongius* sp. nov. was only retrieved partially, approximately 150 base pairs in length. Due to its limited length, this sequence was solely used as a reference for K2P distance analysis and was excluded from other phylogenetic analyses. Consequently, the 28S rRNA dataset was used to construct the ML and BI phylogenetic trees to confirm the phylogenetic position of our species.

The pairwise distance analysis revealed that nine of the Korean *A. (S.) tridentatus* specimens varied in the range from 0 to 0.54% among themselves for the mtCOI region (Table S2). There was no observed variation intraspecifically in pairwise distance for the 18S and 28S rRNA regions (Tables S2 and S3). Single 18S rRNA and 28S rRNA sequences for *A. (S.) tridentatus* were available on NCBI (accession numbers OQ396722 and OQ417523, respectively), both of which were identical to the 18S and 28S rRNA sequences of the Korean *A. (S.) tridentatus*. However, no other molecular sequences from congeneric species were available for assessing congeneric interspecific distances of *Acanthonchus*. In terms of *P. spongius* sp. nov., three specimens exhibited no intraspecific distance among themselves for the 28S rRNA region (Table S4), while their mtCOI intraspecific distance ranged from 0 to 1.09% (Table S2). Intraspecific distance for the 18S rRNA region could not be calculated due to lack of sequences. For congeneric interspecific comparison, a variety of *Paracanthonus* sequences were retrieved from the NCBI (e.g., *P. caecus*, *P. gynodiporata*, *P. macrodon*, *P. yeongjongensis*, *P. miltommatus*, *P. punctatus*, and *P. mamubiae*). An 18S rRNA sequence of *P. wellsii* was excluded from the analysis due to a lack of alignment overlap. The congeneric interspecific distance ranged from 13.6 to 21.8% for the mtCOI region (Table S2). As for the 18S and the 28S rRNA region, the congeneric interspecific distance ranged from 0 to 15.1% (Table S3), and 6.6 to 14.7% (Table S4), respectively. As mentioned previously, only a single very short (~150 bp) 18S rRNA sequence of the new species was obtained and used for comparison. Interestingly, this very short sequence was an exact match to *P. macrodon* and *A. (S.) tridentatus*. However, given its short length, this cannot suggest a close relationship between these species, especially considering that other regions (mtCOI and 28S rRNA) of these two species showed considerable differences (mtCOI region of *P. macrodon* and *A. (S.) tridentatus* differing regarding the new species by 16.2% and 11.7%, respectively) (Tables S2 and S4). Additionally, it is worth mentioning that *P. spongius* sp. nov. exhibited low

interspecific differences with *A. (S.) tridentatus* across all three regions (mtCOI, 18S, and 28S): 11.7%, 0, and 5.8%, respectively (Tables S2–S4).

The BI (Figure 6) and the ML (Figure S1) trees based on the 28S rRNA region possessed identical topology. A total of five species belonging to *Paracanthonchus* (subfamily Paracanthonchinae) were available from GenBank and were consequently used for phylogenetic analysis. Two additional cyatholaimids (belonging to subfamily Cyatholaiminae), *Metacyatholaimus delicatus* and *Praecanthonchus punctatus*, were included to see whether the two subfamilies could be distinguished phylogenetically. In the BI tree, *Metacyatholaimus delicatus* was the most divergent, with 100% pp (Figure 6). *Praecanthonchus punctatus*, the second species belonging to the subfamily Cyatholaiminae, formed a clade with *P. caecus* and *P. yeongjongensis* with 88% pp (Figure 6). *Paracanthonchus spongus* sp. nov. and the Korean *A. (S.) tridentatus* were grouped with the rest of *Paracanthonchus* sequences with 100% pp (Figure 6).

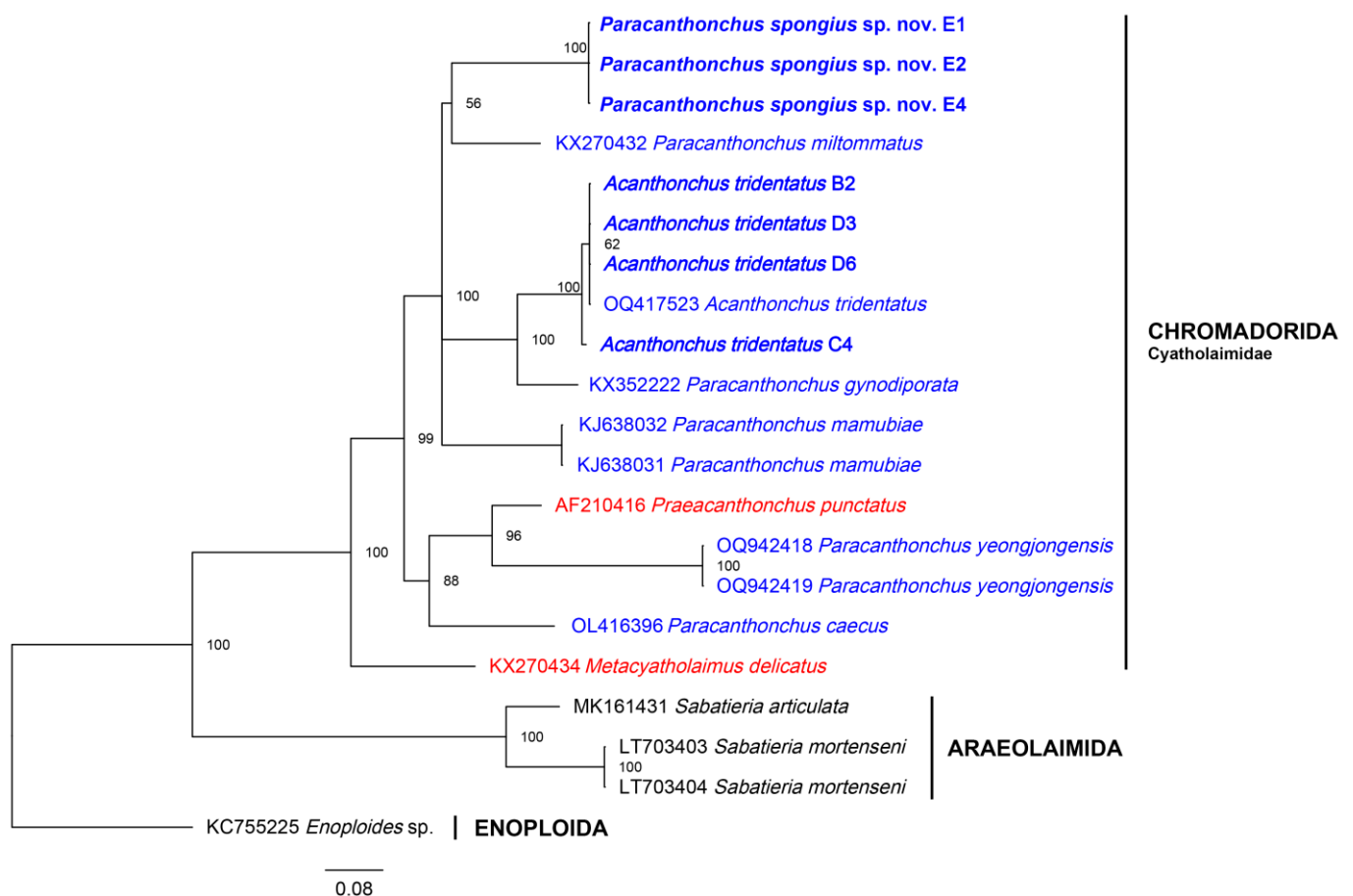


**Figure 6.** A Bayesian inference phylogenetic tree rooted with *Enoploides* sp. as an outgroup, constructed using 28S rRNA gene (with posterior probability as percentage displayed at each node). Specimens from this study are marked in bold, subfamily Cyatholaiminae marked in red, and subfamily Paracanthonchinae marked in blue.

#### 4. Discussion

*Acanthonchus* is a genus with a total of ten valid species classified into two subgenera [39]. It has been reported from various regions around the world, such as Europe, the United States, East Asia, and Southeast Asia. This genus inhabits diverse habitats, including algae, rock pools, and substrates ranging from coarse sand to mud [1,9,32–39]. This genus is part of a very complex family, Cyatholaimidae, composed of 26 genera. The genus has a noticeably distinctive structure, a remarkably large anterior-most supplement compared to other genera of the family, making species identification of the genus relatively straightfor-

ward compared to others. In 1955, Wieser divided the genus (then comprising five species, *A. arcuatus*, *A. cobbi*, *A. setoi*, *A. viviparus*, and *A. gracilis*) into two subgenera, *Acanthonchus* (*Seuratiella*) and *Acanthonchus* (*Acanthonchus*), based on the presence or absence of dorsal teeth [8]. Apart from this differentiating trait, there are no other morphological traits that can be used consistently to distinguish the two subgenera (e.g., presence/absence of ocelli, LD, or number of supplements) (Table 2). In contrast to *Acanthonchus*, an even larger genus belonging to the same family, *Paracanthonchus*, does not utilize dorsal tooth development as an important species-defining morphological trait [8]. Despite consisting of a greater number of species, *Paracanthonchus* does not differentiate subgenera based on the presence or absence of dorsal teeth. Even when he established the subgenera in 1955, he directly expressed that the two subgenera might turn out to be synonymous in the future on account of the character being too minor [8]. Currently, among the ten valid species of *Acanthonchus*, one species remains unclassified within a subgenus. *A. singaporensis*, reported in 2015, was initially reported without a subgenus [9], but, upon checking dorsal teeth through the original description, we are classifying the species under the subgenus *Seuratiella* due to the presence of a small dorsal tooth. The validity of the subgenus is definitely questionable in our opinion but cannot be overturned yet due to a lack of molecular data for this genus (with only one species sequence registered). Sufficient molecular sequences of the genus will need to accumulate to determine whether the subgenera form discernable clades. Only then can we ascertain whether the absence or presence of dorsal teeth is a taxonomically important trait to maintain the validity of the two subgenera. It will also be interesting to observe whether congeneric species form a monophyletic clade around *A. tridentatus*.

The species of *Acanthonchus* (*Seuratiella*) *tridentatus*, reported in this study, was initially regarded as a potential new species during the early stages of the investigation. The Korean *A. (S.) tridentatus* exhibited several morphological similarities to the original description, such as the number and type of preloacal supplement, the shape of spicules and gubernaculum, the number and size of postanal setae, and the size and number of turns in the amphid. Furthermore, molecular sequences (18S and 28S rRNA) from our *A. (S.) tridentatus* showed a 100% match to an entry on NCBI, also identified as *A. (S.) tridentatus* (although the reliability of this species identification remains uncertain). Nevertheless, numerous distinctions between the two species cannot be disregarded. The Korean species and the original species differ in various aspects, such as the body length (1662–1991  $\mu\text{m}$  vs. 833–1358  $\mu\text{m}$ ), the head diameter (21–25  $\mu\text{m}$  vs. 13–19  $\mu\text{m}$ ), the position of the nerve ring (101–123  $\mu\text{m}$  vs. 59–95  $\mu\text{m}$ ), the pharynx length (177–206.5  $\mu\text{m}$  vs. 106–166  $\mu\text{m}$ ) (thus differing in various body ratios), and the presence/absence of the ocelli (present vs. absent). Also, the Korean females exhibit larger overall sizes compared to males, whereas the original species maintains size consistency between genders. Notably, the body size of the Korean species is approximately 1.5 times larger than that of the original species, accompanied by differences in additional morphological traits. As evident from the species name “*tridentatus*”, the species can be distinguished for the three large denticles located beneath the gubernaculum. Upon examining the Korean species, it was confirmed that there are indeed larger denticles present in the lower region of the gubernaculum. However, whether these denticles were present in groups of three was not clear in the Korean specimens. In fact, even species like *Paracanthonchus macrodon* possess a gubernaculum with large denticles underneath, but the number of these denticles is not always consistent [1,13,36]. Whether the species discovered in Korea is part of the morphological variation in *A. (S.) tridentatus* or should be a new species on its own can only be determined by acquiring genetic data of the original species of *tridentatus* (or with species caught from type locality). The voucher specimen of *A. (S.) tridentatus* on NCBI (accession numbers OQ396722 and OQ417523) should also be checked morphologically to see whether such variations exist. Until comprehensive comparisons, validated through both morphological and molecular analyses, distinction of the Korean specimens should be considered as a variation in *A. (S.) tridentatus*.

*Paracanthonchus* is the largest genus within the family Cyatholaimidae, comprising 60 species out of approximately 250 species recorded within the family [2,16]. The large

genus size is supported by its widespread distribution across diverse habitats and geographical regions [1,10]. *Paracanthonchus*, with many other congeners of the family, is defined by a combination of overlapping non-synapomorphic morphological traits. *Paracanthonchus* is the most generic genus of them all, acting almost like a “sanctuary” within the family Cyatholaimidae, accommodating all generic species that are difficult to be classified into any particular genus. To thoroughly organize this genus, substantial molecular data must be established to search for the potential significant morphological traits. The pore complex and lateral pore-like structures have been suggested to be such characters [1,3,4], but most of the preexisting records and description overlook these characters and lack molecular data. Among the sixty valid species recorded, only seven species (*P. yeongjongensis*, *P. wellsi*, *P. miltoammatus*, *P. gynodiporata*, *P. caecus*, *P. macrodon*, and *P. mamubiae*) have their genetic data available in GenBank (albeit with varying marker regions), posing challenges to find taxonomically important traits and re-organize the systematics.

The new species, *Paracanthonchus spongius*, shares generic characteristics, such as a conical buccal cavity with one large dorsal tooth and subventral teeth, tubular pre-cloacal supplements, and a gubernaculum paired with a distal portion extended with numerous denticles. While *P. spongius* exhibits similarities to *P. kamui* in terms of the general shape of the body and gubernaculum, it differs in other aspects, such as the position of amphid (9–12 vs. 6  $\mu\text{m}$  from the anterior end, respectively), ratio of gubernaculum to spicule, and in the number of pre-cloacal supplements (5 vs. 6, respectively). In reference to the tabular key (Table S1) and comparison with species possessing five tubular pre-cloacal supplements (a total of 22 species), the new species is similar to *P. caecus* in the body shape, the spicule length (47–48.5 vs. 40–48), the ratio of spicule to gubernaculum, and the position and size of amphid (9–12  $\mu\text{m}$ , 7.5–10 vs. 10  $\mu\text{m}$ , 7–13  $\mu\text{m}$ ), but it differs by the body length (1793–2145 vs. 976–1470), the position of pre-cloacal supplements, and the shape of the gubernaculum tip.

Our molecular analyses corroborate previous studies, suggesting that the family Cyatholaimidae is indeed monophyletic. *Paracanthonchus* is shown to be distributed in all groups within this monophyletic clade, without distinction based on subfamilies. Granted, only a limited number of sequences were available and used for analysis. *Acanthonchus tridentatus* was positioned within non-monophyletic groups of *Paracanthonchus* (Figure 6). Of the ten valid species of *Acanthonchus*, this is the sole available sequence, which leaves the true relationship of *Acanthonchus* uncertain. Based solely on the results (albeit with very limited sequences), *Acanthonchus* appears to be closely related to the complex of *Paracanthonchus* species (Figures 6 and S1, Tables S2–S4). To establish whether the genus *Acanthonchus* is monophyletic in nature, more sequences from other *Acanthonchus* species will be required.

This represents the first documented instance of a *Paracanthonchus* species found associated with a sponge in an intertidal zone. By providing genetic data and updated morphological descriptions, along with insights into potentially significant morphological traits of the two cyatholaimids discovered in Korea, we are laying the foundation that could be used for the reorganization of this complex family and genus.

**Supplementary Materials:** The following supporting information can be downloaded at: <https://www.mdpi.com/article/10.3390/d15101047/s1>, Figure S1: Rooted maximum likelihood phylogenetic tree of 28S rRNA gene with *Enoploides* sp. set as an outgroup (with UFboot support shown at each node); Table S1: Tabular key of morphological traits of valid *Paracanthonchus* species (amended from Kim, Lee & Jeong, 2023); Table S2: K2P distance between closely related species based on the mtCOI alignment with 1000 bootstrap. Specimens from this study marked bold, with standard deviation marked in blue; Table S3: K2P distance between closely related species based on the 18S rRNA alignment with 1000 bootstrap. Specimens from this study marked bold, with standard deviation marked in blue; Table S4: K2P distance between closely related species based on the 28S rRNA alignment with 1000 bootstrap. Specimens from this study marked bold, with standard deviation marked in blue.

**Author Contributions:** Conceptualization, H.K. and R.J.; methodology, H.K.; software, R.J.; validation, H.K. and R.J.; formal analysis, H.K. and R.J.; investigation, H.K.; resources, H.K. and R.J.; data curation, H.K. and R.J.; writing—original draft preparation, H.K. and R.J.; writing—review and editing, H.K. and R.J.; visualization, H.K. and R.J.; supervision, R.J.; project administration, H.K. and R.J.; funding acquisition, H.K. and R.J. All authors have read and agreed to the published version of the manuscript.

**Funding:** This research was funded by National Institute of Biological Resources (NIBR), funded by the Ministry of Environment (MOE) of the Republic of Korea (NIBR202304103), and by grant (NRF-2021R1I1A1A01040377) from the National Research Foundation of Korea.

**Institutional Review Board Statement:** Not applicable.

**Data Availability Statement:** The voucher specimens examined within this study were deposited to the National Institute of Biological Resources (NIBR), Korea. Partial sequences of mtCOI, 18S, and 28S rRNA were deposited in GenBank. The GenBank accession numbers are listed in Table 1.

**Conflicts of Interest:** The authors declare no conflict of interest. The funders had no role in the design of the study; in the collection, analyses, or interpretation of data; in the writing of the manuscript; or in the decision to publish the results.

## Abbreviations

a	body length divided by maximum body diameter
abd	anal body diameter ( $\mu\text{m}$ )
amp	transversal diameter of amphid ( $\mu\text{m}$ )
amp'	diameter of amphid divided by corresponding body diameter
amp cbd	corresponding body diameter at the level of amphid ( $\mu\text{m}$ )
b	body length divided by esophagus length
bcl	distance from anterior edge to base of buccal cavity
c	body length divided by tail length
c'	tail length divided by anal body diameter
cyln	length of cylindrical tail portion ( $\mu\text{m}$ )
CSL	cephalic sensilla length ( $\mu\text{m}$ )
das	distance from anus to most anterior supplement
dps	distance from anus to most posterior supplement
EL	distance from anterior edge to excretory pore ( $\mu\text{m}$ )
hd	head diameter ( $\mu\text{m}$ )
L	total body length ( $\mu\text{m}$ )
LSL	outer labial sensilla length ( $\mu\text{m}$ )
mbd	maximum body diameter ( $\mu\text{m}$ )
NL	distance from anterior edge to nerve ring ( $\mu\text{m}$ )
na	number of turns in amphid
ns	number of supplements
ncbd	corresponding body diameter at the level of nerve ring ( $\mu\text{m}$ )
PL	pharynx length ( $\mu\text{m}$ )
pcbd	corresponding body diameter at base of pharynx ( $\mu\text{m}$ )
s'	spicule length as arc length divided by anal body diameter
spic	spicule length as arc ( $\mu\text{m}$ )
gub	gubernaculum length as arc ( $\mu\text{m}$ )
TL	tail length ( $\mu\text{m}$ )
V	vulva distance from anterior end divided by total body length
VL	distance from anterior end to vulva ( $\mu\text{m}$ )

## References

1. Cunha, B.P.; Fonseca, G.; Amaral, A.C.Z. Diversity and Distribution of Cyatholaimidae (Chromadorida: Nematoda): A Taxonomic and Systematic Review of the World Records. *Front. Mar. Sci.* **2022**, *9*, 836670. [[CrossRef](#)]
2. Kim, H.; Lee, W.C.; Jeong, R. Molecular Phylogeny of the Genus *Paracanthonus* (Nematoda: Chromadorida) with Description of *P. yeongjogensis* sp. nov. from Korea. *Diversity* **2023**, *15*, 664. [[CrossRef](#)]

3. Leduc, D.; Zhao, Z.Q. Phylogenetic relationships within the Cyatholaimidae (Nematoda: Chromadorida), the taxonomic significance of cuticle pore and pore-like structures, and a description of two new species. *Mar. Biodivers.* **2018**, *48*, 217–230. [[CrossRef](#)]
4. Cunha, B.P.; Fonseca, G.; Amaral, A.C.Z. Two new species of Cyatholaimidae (Nematoda: Chromadorida) from the Southeastern Brazilian coast with emphasis on the pore complex and lateral pore-like structures. *PeerJ* **2023**, *11*, e14712. [[CrossRef](#)] [[PubMed](#)]
5. Tchesunov, A.; García, P.R.; Simakova, U.; Mokievsky, V. *Acanthopharynx* Marine Nematodes (Nematoda, Chromadorida, Desmodoridae) Dwelling in Tropical Demosponges: Integrative Taxonomy with Description of a New Species. *Diversity* **2023**, *15*, 48. [[CrossRef](#)]
6. Bongers, T. Bionomics and reproductive cycle of the nematode leptosomatum bacillatum living in the sponge halichondria panicea. *Neth. J. Sea Res.* **1983**, *17*, 39–46. [[CrossRef](#)]
7. García-Hernández, J.E.; Hammerman, N.M.; Cruz-Motta, J.J.; Schizas, N.V. Associated organisms inhabiting the calcareous sponge *Clathrina lutea* in La Parguera, Puerto Rico. *Caribb. J. Sci.* **2019**, *49*, 239. [[CrossRef](#)]
8. Wieser, W. A Collection of marine nematodes from Japan. *Publ. Seto Mar. Biol. Lab.* **1955**, *4*, 159–181. [[CrossRef](#)]
9. Chen, C.A.; Nguyen, D.T.; Smol, N. Two new free-living marine nematode species from an intertidal sandy-rocky shore on Pulau Ubin, Singapore with a key to the valid species of the genera *Prooncholaimus* and *Acanthonchus*. *Raffles Bull. Zool.* **2015**, (Suppl. S31), 68–74.
10. Miljutina, M.A.; Miljutin, D.M. A revision of the genus *Paracanthochus* (Cyatholaimidae, Nematoda) with a tabular key to species and a description of *P. mamubiae* sp. n. from the deep North-Western Pacific. *Deep Sea Res. Part II Top. Stud. Oceanogr.* **2015**, *111*, 104–118. [[CrossRef](#)]
11. Tchesunov, A. Order Chromadorida Chitwood, 1933. In *Handbook of Zoology*; Schmidt-Rhaesa, A., Ed.; De Gruyter: Berlin, Germany, 2014; pp. 373–398.
12. Tchesunov, A.V. Free-living nematode species (Nematoda) dwelling in hydrothermal sites of the North Mid-Atlantic Ridge. *Helgol. Mar. Res.* **2015**, *69*, 343–384. [[CrossRef](#)]
13. Lee, H.J.; Jung, J.; Rho, H.S. Two unrecorded marine nematode species of *Paracanthochus* (Nematoda: Cyatholaimidae) from the East Sea of Korea. *J. Species Res.* **2016**, *5*, 503–513. [[CrossRef](#)]
14. Hopper, D. Drawing and measuring nematodes. In *Laboratory Methods for Work with Plant and Soil Nematodes*; Ministry of Agriculture, Fisheries and Food; Her Majesty's Stationery Office: London, UK, 1970.
15. Schindelin, J.; Arganda-Carreras, I.; Frise, E.; Kaynig, V.; Longair, M.; Pietzsch, T.; Preibisch, S.; Rueden, C.; Saalfeld, S.; Schmid, B.; et al. Fiji: An open-source platform for biological-image analysis. *Nat. Methods* **2012**, *9*, 676–682. [[CrossRef](#)] [[PubMed](#)]
16. Hodda, M. Phylum Nematoda: A classification, catalogue and index of valid genera, with a census of valid species. *Zootaxa* **2022**, *5114*, 1–289. [[CrossRef](#)]
17. Platt, H.; Warwick, R. *Free-Living Marine Nematodes*; Part 2: British Chromadorids; Linnean Society of London: London, UK, 1988; p. 502.
18. Derycke, S.; Vanaverbeke, J.; Rigaux, A.; Backeljau, T.; Moens, T. Exploring the Use of Cytochrome Oxidase c Subunit 1 (COI) for DNA Barcoding of Free-Living Marine Nematodes. *PLoS ONE* **2010**, *5*, e13716. [[CrossRef](#)] [[PubMed](#)]
19. Carta, L.K.; Li, S. Improved 18S small subunit rDNA primers for problematic nematode amplification. *J. Nematol.* **2018**, *50*, 533–542. [[CrossRef](#)] [[PubMed](#)]
20. Carta, L.K.; Li, S. PCR amplification of a long rDNA segment with one primer pair in agriculturally important nematodes. *J. Nematol.* **2019**, *51*, e2019-26. [[CrossRef](#)]
21. De Ley, P.; De Ley, I.T.; Morris, K.; Abebe, E.; Mundo-Ocampo, M.; Yoder, M.; Heras, J.; Waumann, D.; Rocha-Olivares, A.; Burr, A.J.; et al. An integrated approach to fast and informative morphological vouchering of nematodes for applications in molecular barcoding. *Philos. Trans. R. Soc. B Biol. Sci.* **2005**, *360*, 1945–1958. [[CrossRef](#)]
22. Thompson, J.D.; Higgins, D.G.; Gibson, T.J.; Clustal, W. Improving the Sensitivity of Progressive Multiple Sequence Alignment through Sequence Weighting, Position-Specific Gap Penalties and Weight Matrix Choice. *Nucleic Acids Res.* **1994**, *22*, 4673–4680. [[CrossRef](#)]
23. Tamura, K.; Stecher, G.; Kumar, S. MEGA11: Molecular Evolutionary Genetics Analysis Version Mol. *Biol. Evol.* **2021**, *38*, 3022–3027. [[CrossRef](#)]
24. Minh, B.Q.; Schmidt, H.A.; Chernomor, O.; Schrempf, D.; Woodhams, M.D.; von Haeseler, A.; Lanfear, R. IQ-TREE 2: New Models and Efficient Methods for Phylogenetic Inference in the Genomic Era. *Mol. Biol. Evol.* **2020**, *37*, 1530–1534, Erratum in *Mol. Biol. Evol.* **2020**, *37*, 2461. [[CrossRef](#)]
25. Altschul, S.F.; Gish, W.; Miller, W.; Myers, E.W.; Lipman, D.J. Basic local alignment search tool. *J. Mol. Biol.* **1990**, *215*, 403–410. [[CrossRef](#)] [[PubMed](#)]
26. Kimura, M. A simple method for estimating evolutionary rates of base substitutions through comparative studies of nucleotide sequences. *J. Mol. Evol.* **1980**, *16*, 111–120. [[CrossRef](#)] [[PubMed](#)]
27. Minh, B.Q.; Nguyen, M.A.T.; Von Haeseler, A. Ultrafast Approximation for Phylogenetic Bootstrap. *Mol. Biol. Evol.* **2013**, *30*, 1188–1195. [[CrossRef](#)]
28. Kalyaanamoorthy, S.; Minh, B.Q.; Wong, T.K.F.; Von Haeseler, A.; Jermini, L.S. ModelFinder: Fast model selection for accurate phylogenetic estimates. *Nat. Methods* **2017**, *14*, 587–589. [[CrossRef](#)]

29. Darriba, D.; Taboada, G.L.; Doallo, R.; Posada, D. jModelTest 2: More models, new heuristics and high-performance computing. *Nat. Methods* **2012**, *9*, 772. [[CrossRef](#)] [[PubMed](#)]
30. Huelsenbeck, J.P.; Ronquist, F. MRBAYES: Bayesian inference of phylogenetic trees. *Bioinformatics* **2001**, *17*, 754–755. [[CrossRef](#)] [[PubMed](#)]
31. Rambaut, A. *FigTree*, Version 1.4.4.; Institute of Evolutionary Biology, University of Edinburgh: Edinburgh, UK, 2018.
32. Kreis, H.A. Weiterer Beitrag zur Kenntnis der Freilebenden Marinen Nematoden. *Arch. Naturgeschichte* **1928**, *92*, 1–29.
33. Chitwood, B.G. North American marine nematodes. *Tex. J. Sci.* **1951**, *3*, 617–672.
34. Wieser, W. Free-living nematodes and other small invertebrates of Puget Sound beaches. *Univ. Wash. Publ. Biol.* **1959**, *19*, 1–179.
35. Cobb, N.A. One hundred new nemas (type species of 100 new genera). *Contrib. Sci. Nematol.* **1920**, *9*, 217–343.
36. Ditlevsen, H. Marine Freelifving Nematodes from Danish Waters. *Vidensk. Meddr. Dan. Naturh. Foren.* **1918**, *70*, 147–214.
37. Vitiello, P. Nématodes libres marins des vases profondes du Golfe du Lion. II. Chromadorida. *Téthys* **1970**, *2*, 449–500.
38. Kito, K. Studies on the free-living marine nematodes from Hokkaido, IJ. *Fac. Sci. Hokkaido University. Ser. VI Zool.* **1976**, *20*, 568–578.
39. NemysEds. Nemys: World Database of Nematodes. 2023. Available online: <https://nemys.ugent.be> (accessed on 1 April 2023).

**Disclaimer/Publisher’s Note:** The statements, opinions and data contained in all publications are solely those of the individual author(s) and contributor(s) and not of MDPI and/or the editor(s). MDPI and/or the editor(s) disclaim responsibility for any injury to people or property resulting from any ideas, methods, instructions or products referred to in the content.